The Exceptional Hydrogen-Bond Properties of Neutral and Protonated Lobeline

Abel Locati,[†] Michel Berthelot,[†] Michel Evain,[‡] Jacques Lebreton,[§] Jean-Yves Le Questel,[†] Monique Mathé-Allainmat,[§] Aurélien Planchat,[†] Eric Renault,[†] and Jérôme Graton*[,†]

Laboratoire de Spectrochimie et Modélisation (EA 1149, FR 2465), Laboratoire de Chimie du Solide (Institut Jean Rouxel, CNRS UMR 6502), Laboratoire de Synthèse Organique (CNRS UMR 6513, FR 2465), Université de Nantes, Nantes Atlantique Universités, Faculté des Sciences et des Techniques de Nantes, 2, rue de la Houssinière, BP 92208, F-44322 Nantes Cedex 3, France

Received: February 28, 2007; In Final Form: May 10, 2007

The X-ray diffraction structure of (−)-lobeline, a high affinity nicotinic ligand, has been determined. A comparison with its hydrobromide and hydrochloride salts shows the great flexibility of the two lateral chains of the *N*-methylpiperidine ring. Infrared studies carried out on the same species, in the solid state and in solution, reveal the propensity of this molecular framework to accommodate very specific hydrogen bonds (HBs) depending on the state—neutral or protonated—of the molecule. In solution, a strong internal HB between the hydroxyl group and the piperidine nitrogen gives an exceptionally high HB affinity to the hydroxyl oxygen of the lobeline base. In the ionic form, both NH^+ and OH groups of the molecule cooperate as HB donors to chelate the counterion. These interactions provide very stable structures and indicate that protonated lobeline can also act as a strong HB donor.

I. Introduction

The recent isolation of different acetylcholine binding proteins (AChBP)[1,2] has had a considerable impact in the characterization of the ligand recognition site of the nicotinic acetylcholine receptors (nAChRs). For example, the experimental measurement of the global energy of the ligand docking has become accessible.[3] In addition, the structural resolution of the AChBP complexes with nicotinic ligands[3,4] has revealed the spatial disposition of the agonist toward the different residues of the protein. This information has been used to build molecular models thus enabling preliminary estimations of the energies of the multiple interactions involved in the recognition process. Up to now, only a limited number of complexes have been analyzed, compared to the wide variety of structures of the nAChRs ligands. Despite the increased efforts devoted to the development of accurate theoretical tools for the investigation of protein−ligand interactions, a thorough understanding of the ligand conformational features constitutes an important prerequisite. Moreover, the reliability of the separation of the global experimental docking energies into the different individual ligand−receptor interactions depends on the effective localization of the active sites of the ligand and on the exact calibration of their strength by reference to experimental values. As part of our program on the determination of the HB accepting and donating characteristics of nAChRs ligands,[5−9] we initiated a project directed toward the elucidation of the structure of the most important nicotinic agonists in their neutral and charged forms. Among these agonists, (−)-lobeline is a high affinity ligand with an inhibition constant K_i in the nanomolar range.[10,11] While lobeline definitely shows nicotine-like behavior such as anxiolytic and antinociceptive effects or enhancement of cognitive performance, its pharmacological profile appears particularly complex[12] and it may be presented as an agonist[13] or an antagonist[14] of nicotine toward nAChRs. These properties suggest either a specific interaction with the nicotinic receptor or a possible docking on another receptor subtype followed by indirect agonist effects.[15,16] It has also been found that lobeline causes the release of serotonin and dopamine in the synaptic cleft indicating several potential therapeutic activities in the whole neuronal network.[17,18] The structure of (−)-lobeline **1a** consists of an *N*-methylpiperidine ring flanked in the 2 and 6 positions by two flexible arms containing in β position a carbonyl and a hydroxyl group, respectively. The presence of these two lateral chains and the trisubstitution of the piperidinic ring generate a great number of possible conformers.

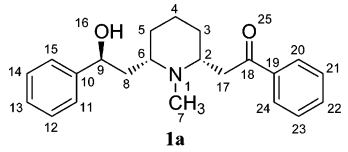

1a

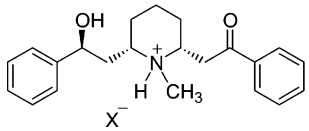

2 (X = Cl), **3** (X = Br), **4** (X = I)

The structure−affinity investigations carried out by Flammia et al. on 19 lobeline analogues[10] showed that the two oxygenated arms contribute to the high affinity of lobeline for the $\alpha 4\beta 2$ receptor subtype. Removal of either one or both oxygen functions led to significant decrease in the binding affinity for rat brain nAChRs. The unique (still unexplained) exceptions correspond to the compound where the hydroxyl group is substituted by a chlorine atom[10] or tosylate,[19] which bind with the same affinity as lobeline itself. The structural analyses of

* Corresponding author. E-mail: jerome.graton@univ-nantes.fr. Tel: 332 51 12 55 71. Fax: 332 51 12 55 67.
† Laboratoire de Spectrochimie et Modélisation (EA 1149, FR 2465).
‡ Laboratoire de Chimie du Solide (Institut Jean Rouxel, CNRS UMR 6502).
§ Laboratoire de Synthèse Organique (CNRS UMR 6513, FR 2465).

10.1021/jp071632b CCC: $37.00
Published on Web 06/23/2007

the affinities of the nAChR ligands generally refer to the Beers and Reich[20] or Sheridan[21] phamacophore models, which stipulate that the minimum requirement for the affinity is the presence of a HB acceptor site about 4.8 Å distant from a cationic ammonium center. In the lobeline molecule ($pK_a = 8.6$)[22] which is 90% protonated at physiological pH, there are two candidates for the HB accepting centers: the carbonyl and the hydroxyl functional groups. Both are weak acceptors (acetophenone: $pK_{HB} = 1.11$;[23] benzyl alcohol: $pK_{HB} = 0.86$)[24] and may be placed by rotation around the single bonds at an acceptable distance from the ammonium nitrogen. It has been generally assumed, on the basis of geometrical arguments, that the carbonyl oxygen is the accepting group in lobeline.[10,22,25] A clear confirmation of this hypothesis has been afforded by the structure of lobeline in the ligand-binding pocket of AChBP.[4] The solid-state structure of lobeline hydrochloride monohydrate was established by Barlow and Johnson.[22] Glaser et al.[25] reported later the X-ray structure of the hydrobromide. In both crystal units, the *N*-methylpiperidine ring is in a chair conformation with an axial *N*-methyl position. The main difference between the two structures stems from the β-hydroxyphenethyl arm which is rotated around the C_6-C_8 bond so that the hydrated hydrochloride presents an internal HB $N^+H\cdots OH$ whereas the lobeline hydrobromide forms intermolecular $\cdots Br^-\cdots H\text{-}N^+$ O-H$\cdots Br^-\cdots$ hydrogen bonds. In a detailed ^{13}C and ^1H NMR analysis, Glaser et al.[25] obtained very important information about the structure of neutral and protonated lobeline. They detected the presence of minor amounts of the equatorial *N*-methyl diastereoisomer, and they found that the most stable rotational isomers of the two arms always corresponded to species containing internal HBs. On the basis of molecular mechanics calculations, the N^+H hydrogen of the hydrochloride may be hydrogen-bonded to the OH or to the C=O group but in the neutral form, the hydroxyl group may be connected both to the nitrogen atom and the carbonyl group in a bifurcated HB (structure 1b).

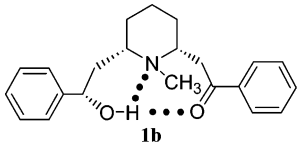

1b

While this study gives a comprehensive picture on the cation structure in different solvents, it does not provide any information about the strongest interaction guiding the overall ion pair structures: the anion−cation interaction. Moreover, the structure of the neutral base needs further investigation since Compère et al.[26] observed, starting from (−)-lobeline, the progressive appearance in $CDCl_3$ of a novel signal attributed to the trans species differing in the axial/equatorial position of the phenacyl arm. This isomerization reaction, confirmed later by Felpin[27] and Zheng,[13] was not detected by Glaser in similar solvents.

In this paper, we present the crystal structure of lobeline base and compare it to the structure of its salts. Second, the infrared spectra of lobeline and its hydrochloride, hydrobromide, and hydroiodide salts are studied. The analysis of these data throws light on the molecular interactions occurring in these various species in the solid state and in carbon tetrachloride or dichloromethane solutions, and their interpretation focuses on their multiple internal and external HBs. Finally, the global HB affinity of lobeline base is measured in solution using 4-nitrophenol as donor, and the contributions of the different individual basic sites are evaluated. These experimental results are supported by DFT and local MP2 theoretical calculations.

II. Experimental and Theoretical Methods

Chemicals. (−)-Lobeline **1** was purchased under its hydrochloride form **2** from Aldrich. It was neutralized by adding an excess of ammonium hydroxide to a distilled water solution (1 g in 150 mL) of the hydrochloride. Neutral lobeline was not soluble in water and precipitated immediately. It was then extracted three times with dichloromethane. A sample suitable for X-ray crystallography of (−)-lobeline **1** was prepared by slow evaporation of the solvent under reduced pressure (100 mbar), then mounting it at the tip of a Lindemann capillary using solvent-free glue, and then transferring it to the cold gas stream of the diffractometer. An additional drying was carried out under higher vacuum (0.1 mbar) for the infrared studies. Neutral lobeline was dissolved in hydrobromic or hydroiodic acid solutions to synthesize the corresponding salts **3** and **4**, respectively. These salts were extracted three times with dichloromethane, and the samples were dried under high vacuum after evaporation of the solvent. The commercial hydrochloride powder was as well carefully dried under high vacuum. The spectroscopic grade solvents were dried over molecular sieves and/or passed through a column of activated basic alumina.

β-*N*,*N*-Dimethylaminopropiophenone (DAPone) hydrochloride was purchased from Aldrich. It was neutralized by reaction with an excess of sodium hydroxide. It was then extracted three times with dichloromethane. The solvent was removed under vacuum, and DAPone was carefully dried under high vacuum. β-*N*,*N*-Dimethylamino-1-phenylpropan-1-ol (DAPol) was synthesized by reduction of DAPone with $NaBH_4$ in aqueous solution at room temperature for 12 h. The treatment of the solution with hydrochloride acid (37%) followed by sodium hydroxide (5N) was carried out to extract the boronate salts and to neutralize DAPol. The solvents were evaporated, and DAPol was carefully dried under high vacuum.

IR Spectra. Data were recorded with a Bruker Tensor 27 FTIR spectrometer at a resolution of 1 cm^{-1}. An Infrasil quartz cell of 1 cm path length and KBr cells of 1 mm and 0.2 mm path lengths were used for the studies of dilute solutions of neutral lobeline and lobeline hydrochloride, hydrobromide, and hydroiodide. For the solid state analysis, spectra were recorded either on hexachlorobutadiene and nujol mulls or on KBr pellets. Thermodynamic measurements on the model compounds were obtained from the decrease in intensity of the OH absorption of *p*-fluorophenol (*p*FP; $\nu(OH) = 3614$ cm^{-1}; $\epsilon = 237$ dm^3 mol^{-1} cm^{-1}) in dilute ternary *p*FP-base-CCl_4 solutions, with the standard procedure used to define the reference pK_{HB} scale of hydrogen bonding.[28] In the cases of lobeline and DAPol, the measurements were carried out using *p*-nitrophenol (*p*NP; ν-(OH) = 3595 cm^{-1}; $\epsilon = 284$ dm^3 mol^{-1} cm^{-1}) as HB donor. This phenol was selected to prevent the superposition of the probe signal with the unchelated OH absorption of the acceptors which occurs at about 3620 cm^{-1}. The linear free energy relationships (LFERs) developed by Abraham et al.,[29,30] may be used to derive eq 1 so that the transformations of the p*K* values in the two scales are straightforward.

$$pK_{HB} = 0.763 \log K(p\text{NP}) - 0.259 \qquad (1)$$

When the basicity measurement is carried out on polybasic compounds or on different species in equilibrium, the decrease in absorbance of the OH vibration band is due to the sum of the various associations at the different sites of the same

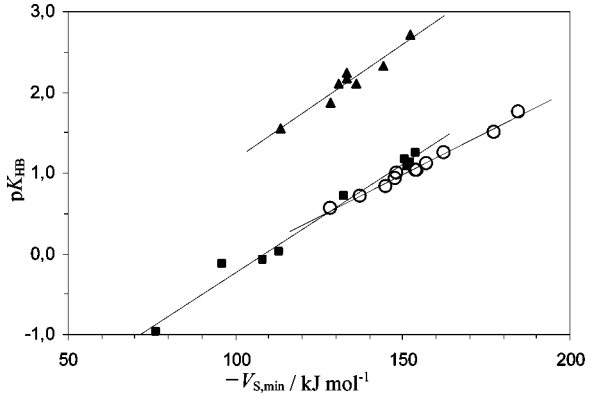

Figure 1. Family dependent relationship between pK_{HB} and $(-V_{S,min})$. Accepting groups: (▲) tertiary amine nitrogen, (■) hydroxyl oxygen, and (○) acetophenone oxygen.

TABLE 1: Reference Compounds Selected for the $pK_{HB}-V_{S,min}$ Calibration Lines in Hydroxyl, Acetophenone, and Tertiary Amine Families

family	compounds	$V_{S,min}$ kJ mol^{-1}[a]	pK_{HB}
hydroxyls	*i*-propanol	−151.3	1.08
	c-hexanol	−152.2	1.14
	1-phenylpropan-1-ol	−132.4	0.71
	1,1,1,3,3,3-hexafluoroisopropanol	−76.4	−0.96
	t-butanol	−150.8	1.17
	adamantan-1-ol	−154.1	1.26
	p-fluorophenol	−96.1	−0.13
	p-methylphenol	−113.2	0.03
	phenol	−108.3	−0.07
acetophenones	*p*-nitroacetophenone	−128.3	0.56
	m-trifluoromethylacetophenone	−138.1	0.72
	m-fluoroacetophenone	−145.1	0.83
	p-chloroacetophenone	−147.7	0.93
	p-fluoroacetophenone	−148.4	1.00
	propiophenone	−153.8	1.04
	butyrophenone	−154.5	1.04
	acetophenone	−157.1	1.11
	p-methylacetophenone	−162.6	1.25
	p-aminoacetophenone	−177.2	1.50
	p-dimethylaminoacetophenone	−184.5	1.76
tertiary amines	*N*-methylmorpholine	−113.4	1.55
	N-methylpiperidine	−131.0	2.11
	trimethylamine	−136.2	2.11
	N,*N*-dimethylethylamine	−133.3	2.17
	N,*N*-dimethylpiperazine	−128.5	1.88
	N-methylpyrrolidine	−133.4	2.25
	quinuclidine	−152.3	2.71
	diazabicyclooctane	−144.3	2.33

[a] B3LYP/6-31+G(d,p).

molecule and/or on the multiple isomers. In these situations, it can easily be demonstrated that the apparent equilibrium constant K_{app} measured by the standard method is the sum of the equilibrium constants K_i on the different sites i, weighted by their fractional population p_i in solution. The important condition is that the solutions are diluted enough so that only 1:1 complexes are present in solution (eq 2).[31,32]

$$K_{app} = \sum_i p_i.K_i \qquad (2)$$

It must be stressed that all the thermodynamic calculations, such as the donor conversions by means of eq 1, are strictly restricted to monofunctional compounds.[31,32] Therefore, specific methods must be developed for polybasic molecules to obtain the individual basicities of their different accepting sites.

Crystal Data for Lobeline Base. Crystal data: $C_{22}H_{27}NO_2$, $M = 337.5$, monoclinic, $a = 17.0284(5)$, $b = 7.0094(4)$, $c = 7.7824(10)$ Å, $\beta = 99.499(5)°$, $V = 916.16(13)$ Å^3, $T = 120$ K, space group $P2_1$ (No. 4), $Z = 2$, μ(Mo Kα) = 0.077 mm^{-1}, 26337 reflections measured, 5111 unique ($R_{int} = 0.096$) which were used in all calculations (4340 observed at a $2\sigma(I)$ level, 229 parameters). The final $wR(F^2)$ was 0.1251 (all data).

Computational Methods. Theoretical calculations were performed using Gaussian 03[33] and Jaguar[34] packages. Owing to the great flexibility of lobeline and certain model molecules, no attempt was made to investigate the whole potential energy surface of the molecules under study. Specific conformations of lobeline suggested by the NMR analyses or the X-ray structures were optimized using the DFT with the B3LYP functional at the 6-31+G(d,p) level of theory. It is well-known that the estimation of the intramolecular basis set superposition error (BSSE) is a difficult task, and it is therefore almost always ignored in the calculations.[35] Lobeline, as well as DAPol, is likely to show stable conformations including intramolecular interactions, and the uncorrected energies lead to an overstabilization of the chelated structures. Consequently, single-point calculations were carried out at the LMP2/6-311++G(d,p)// B3LYP/6-31+G(d,p) level of theory, since the local MP2 (LMP2) method greatly reduces the BSSE contribution.[36]

The hydrogen-bond basicity has been shown[37] to be quantitatively related to the most negative electrostatic potential computed on the molecular surface calculated at the electron density 0.001 e bohr^{-3} provided that the different accepting centers are treated separately.[38,39] All the electrostatic potentials were calculated using the Molden interface[40] from B3LYP/6-31+G(d,p) Gaussian wavefunctions. In this work, the three relevant families of accepting centers are the acetophenone carbonyl oxygen, the hydroxyl oxygen, and the amino nitrogen. The minimum electrostatic potential values of reference compounds for these three families are presented in Table 1. In all series, some bases may be present under several conformations of relatively close energy but with different $V_{S,min}$ values. These values are therefore weighted by a Boltzmann function based on the electronic energy of the isomers. The final $V_{S,min}$ and pK_{HB} data for reference compounds are gathered in Table 1, and Figure 1 shows the family dependent behavior of these properties. This calibration leads to eqs 3−5 for the hydroxyl, acetophenone, and tertiary amine families, respectively.

$$pK_{HB} = -0.0270\, V_{S,min}(OH) - 2.932 \qquad r = 0.992,\ n = 9,\ s = 0.11 \quad (3)$$

$$pK_{HB} = -0.0209\, V_{S,min}(C{=}O) - 2.151 \qquad r = 0.994,\ n = 11,\ s = 0.04 \quad (4)$$

$$pK_{HB} = -0.0285\, V_{S,min}(N) - 1.677 \qquad r = 0.965,\ n = 8,\ s = 0.10 \quad (5)$$

III. Results and Discussion

1. The Solid State of Lobeline and Its Salts. *Infrared Spectra.* The OH, NH^+, and CO stretching are the three characteristic vibrations to be analyzed in the IR spectra of these species. Their positions are reported in Table 2. For the neutral base, a single, intense, and sharp ($\Delta\nu_{1/2} \approx 5$ cm^{-1}) carbonyl absorption is measured at 1686.4 cm^{-1}. Second, a broad and structured band appears at about 3100 cm^{-1} ($\Delta\nu_{1/2} \approx 200$ cm^{-1}). This latter absorption is attributed to the stretching mode of the hydroxyl group involved in an HB interaction. The frequency shift of this band calculated from the hypothetical free OH

TABLE 2: Wavenumbers of the Main Absorptions of Lobeline and Its Salts in the Solid State

no.	compound	ν_{OH} cm^{-1}	ν_{NH^+} cm^{-1}		$\nu_{C=O}$ cm^{-1a}	
1	lobeline base	3115			1686.4	
2	lobeline, H^+Cl^-	3340[b]	2535[c]		1684.3 (8%)	1677.0 (92%)
3	lobeline, H^+Br^-	3375[b]	2635[c]		1685.0 (44%)	1677.4 (56%)
4	lobeline, H^+I^-	3401[b]	2710[c]	1694.1 (17%)	1687.7 (83%)	

[a] Percentage of area between brackets. [b] The shape of the band is distorted by the presence of the harmonic $2\nu_{C=O}$. [c] Approximate position of the center of the multiplet.

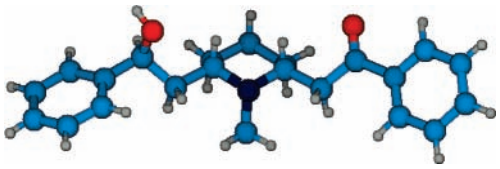

Figure 2. Lobeline base monomer observed in the crystal structure.

Figure 3. Superposition of the crystalline structures of lobeline and its salts. For the sake of clarity, most of hydrogen atoms are not shown.

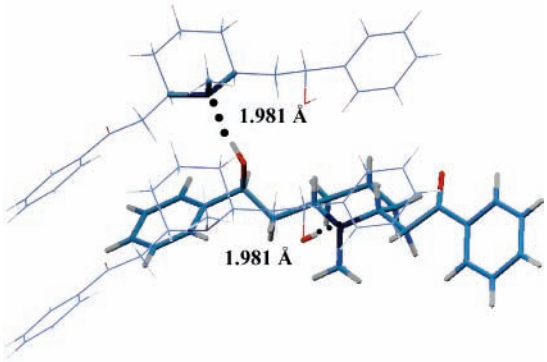

Figure 4. Intermolecular hydrogen-bond network observed in the crystal structure of lobeline base. The central molecule and the groups of the neighboring molecules involved in the hydrogen bonds are shown in stick model.

absorption ($\Delta\nu_{OH} \approx 500$ cm^{-1}) unquestionably corresponds to an association with a tertiary amine nitrogen[41] rather than to a complex with a carbonyl oxygen.[23]

The three salts exhibit the classical structured NH^+ absorption of tertiary ammonium cations and the centroid of the multiplet is, as expected, clearly displaced toward higher frequencies when the anion becomes less basic.[42] The position of the OH stretching bands as well as the shift from one salt to the other, also reveals an association of the type $OH\cdots X^-\cdots HN^+$, where the basicity of the anion is reduced by the hydrogen bond with the protonated amine (vide infra). On the IR spectra, there is however no means to discriminate between an internal HB where the NH^+ and the OH groups of the same molecule form a chelate with the anion and an external HB involving two different molecules of protonated lobeline. Unexpectedly, the carbonyl absorptions of the three salts are split into two bands. A possible interpretation is that the doublet may arise from a Fermi resonance with a harmonic or combination level.[43,44]

X-ray Diffraction Study. The main structural characteristics of lobeline base **1** are illustrated in Figure 2 and reported in the Supporting Information section in addition to the corresponding data for the protonated structures **2** and **3**.[22,25] The piperidinic ring adopts a chair conformation and the *N*-methyl substituent is found in the axial position as in the two salts. The values of the φ dihedral angles relative to the carbonyl moiety, near 180°, indicate a zigzag conformation of an unfold residue. Similar behavior is observed in the hydrobromide **3** and, to a lesser extent, in the hydrochloride **2**. However, in this latter structure, the carbonyl group has lost its conjugation with the aromatic ring: φ (20−19−18−25) = 37.6°, whereas the values are very near 0° in **1** and **3**. The zigzag conformation is also found for the β-hydroxyphenethyl residue in **1** and **3**, while a rotation of about 120° occurs around the C_6-C_8 bond in **2**. Therefore, neutral lobeline **1** and its hydrobromide salt **3** exhibit very similar conformations, which differ significantly from the hydrochloride one, possibly disturbed by the presence of a water molecule in the crystal (vide infra). The superposition of the three structures and the calculation of associated root-mean-square (rms) deviations confirm this qualitative observation. Neutral lobeline **1** is selected as the reference structure, and the piperidine ring is selected as the starting residue to fit. The seven heavy atoms of the *N*-methylpiperidinyl residue fit very well with their counterparts in each salt (0.027 and 0.054 Å for the fitting with **2** and **3**, respectively). The addition of the nine heavy atom pairs of the β-hydroxyphenethyl moieties leads to significant deviations of the rms values in both lobeline hydrochloride (0.778 Å) and lobeline hydrobromide (0.735 Å). In contrast, the consideration of the phenacyl arm provides a better superposition of the structures, especially for the hydrobromide salt (0.096 Å). The greater deviation (0.337 Å) observed between **1** and **2** is mainly explained by the loss of conjugation between the carbonyl and the phenyl groups. For the three structures, Figure 3 shows the superposition of the 16 pairs of heavy atoms of the *N*-methylpiperidinyl and phenacyl residues.

The molecular packing of **1**, organized in sheets, is shown in Figure 4. The molecules are packed along an infinite network of intermolecular $O-H\cdots N$ hydrogen bonds, preferred to cyclic hydrogen-bonded dimers or to internal HBs. As suggested by the infrared results, the nitrogen atom is the only HB acceptor site among the three potential sites of **1** (N_1, O_{16}, and O_{25}). This network provides two equivalent HB interactions $N\cdots H-O$ and $O-H\cdots N$ per lobeline molecule, which are characterized by $d_{N\cdots O} = 2.822$ and $d_{N\cdots H} = 1.981$ Å corresponding to a significant reduction of about 25% of the sum of Bondi's van der Waals radii ($H = 1.10$ and $N = 1.55$ Å).[45] The $O-H\cdots N$ angle (174°) is just slightly distorted from linearity. This molecular packing is very similar to that of the hydrobromide crystal where the bromide anion is just included between the ammonium group of a protonated lobeline and the hydroxyl group of the neighboring molecule, giving two strong $N^+-H\cdots Br^-$ and $O-H\cdots Br^-$ interactions ($d_{H\cdots Br-} = 2.195$ and 2.293 Å, respectively), also at about 75% of the sum of van der Waals radii. A careful examination of the carbonyl environment also reveals a weak $\pi\cdots\pi$ interaction between the electron-rich aromatic ring of the hydroxyl moiety of a first molecule and the electron-depleted π system of the phenacyl arm of the neighboring molecule. The $C\cdots C$ distance (3.30 Å) is slightly

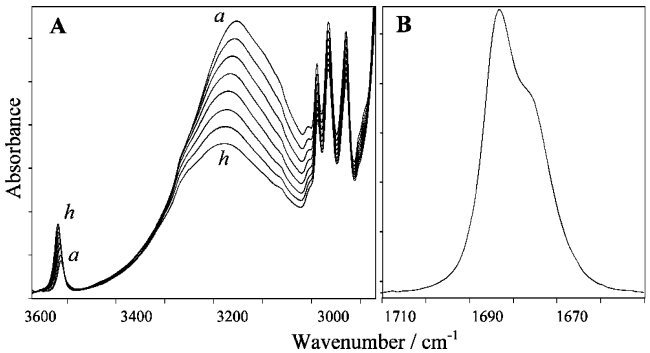

Figure 5. Hydroxyl and carbonyl absorptions of diluted C_2Cl_4 solutions of lobeline (5.10^{-3} dm^3 mol^{-1}): (A) temperature dependence from −5 (*a*) to +100 °C (*h*) of the hydroxyl IR absorptions; (B) $\nu_{C=O}$ absorption band.

less than the sum of the Bondi's van der Waals radii of two carbon atoms ($C = 1.7$ Å).

2. Lobeline and Its Salts in Solution. *Lobeline Base.* The IR spectrum, recorded at 298 K, of neutral lobeline in solution in CCl_4 contains a sharp band at 3616 cm^{-1} ($\Delta\nu_{1/2} = 16$ cm^{-1}) and an intense broad band at 3257 cm^{-1} ($\Delta\nu_{1/2} \cong 260$ cm^{-1}) in the ν(OH) region, indicating the presence of free and hydrogen-bonded species in substantial amounts. Their intensity ratio is not affected by a concentration change under 10^{-2} molar suggesting that the auto association of lobeline no longer occurs. Therefore, the two absorptions can be safely attributed to the existence of an equilibrium (eq 6) between an open form **1a** and a chelated structure. This intramolecular interaction may happen either with the carbonyl oxygen or with the piperidinic nitrogen, but the frequency shift ($\Delta\nu$(OH) = 359 cm^{-1}) definitely discriminates in favor of an association on the nitrogen site **1c**.[23,41]

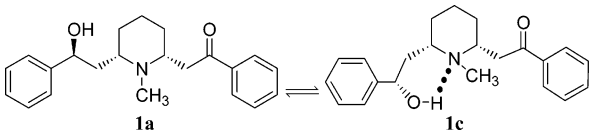

1a ⇌ **1c** (6)

The evolution of the integrated intensity ratio of the two bands with temperature (Figure 5A) leads to an estimation of the equilibrium constant, and thus to the relative populations of the chelated and open lobeline. As proposed by Hartman et al.[46] this constant is written (eq 7) as a function of integrated intensities B and integrated absorption coefficients α. These coefficients α are unknown, but one can check that their ratio is independent of temperature as it corresponds to the slope of relation eq 8, where ℓ is the cell path length and c_T the molar concentration of lobeline.

$$K = \frac{[\text{chelated lobeline}]}{[\text{open lobeline}]} = \frac{B_{chel}}{B_{open}} \frac{\alpha_{open}}{\alpha_{chel}} \quad (7)$$

$$B_{chel} = -\frac{\alpha_{chel}}{\alpha_{open}} B_{open} + \alpha_{chel}/c_T \quad (8)$$

The equilibrium constant K can then be determined at several temperatures, and the thermodynamics of the reaction can be deduced from the van't Hoff equation. In this study, the infrared spectra of lobeline in solution in CCl_4 and C_2Cl_4 were recorded at various temperatures from −5 to +55 °C and from −5 to +100 °C, respectively (Figure 5A). The integrated absorption coefficient ratio was indeed found to be independent of the temperature variation, as shown by the statistics of eq 9 obtained from C_2Cl_4 data. The thermodynamic parameters of the equilibrium were deduced from the van't Hoff equation and are reported in Table 3.

TABLE 3: Thermodynamics of the Chelation Equilibrium of Lobeline in Solution

solvent	CCl_4	C_2Cl_4
$\Delta H^{\circ a}$	−12.0	−15.0
$\Delta S^{\circ}_{298}{}^{b}$	−28	−36
$\Delta G^{\circ}_{298}{}^{a}$	−3.7	−4.1
K_{298}	4.4	5.3
$p_i{}^{c}$	81%	84%

[a] kJ mol^{-1}. [b] J mol^{-1} K^{-1}. [c] Population of the chelated form.

TABLE 4: Relative Energies and in Vacuo Populations of Lobeline Conformers from B3LYP and LMP2 Methods

		chelated forms		open forms[a]	
conformer		**1c**	**1b**	**1a**	**1a′**
ΔE_{el} (B3LYP)[b,c]		0.0	7.1	13.0	16.1
$p_i{}^{d}$		94.0%	5.3%	0.5%	0.1%
ΔE_{el} (LMP2)[c,e]		0.0	3.4	2.8	10.9
$p_i{}^{d}$		62.7%	16.1%	20.4%	0.8%
$\bar{V}_{S,min}{}^{c}$	OH	−171.4		−140.2	
	C=O	−134.6		−141.9	

[a] Two stable open structures denoted **1a** and **1a′** are found (see Supporting Information). They mainly differ by the rotation of the hydroxyphenethyl arm. [b] B3LYP/6-31+G(d,p)// B3LYP/6-31+G(d,p) level. [c] kJ mol^{-1}. [d] Boltzmann population. [e] LMP2/6-311++G(d,p)// B3LYP/6-31+G(d,p) level.

$$B_{chel} = -21.0\, B_{open} + 214.2; \quad n = 8;\ r^2 = 0.993;\ s = 1.75 \quad (9)$$

These values can be compared to the thermodynamics of the association of methanol (a slightly weaker donor than benzyl alcohol)[30] with *N*-methylpiperidine in C_2Cl_4 ($K_{298} = 51$; $\Delta G^{\circ}_{298} = -9.7$ kJ mol^{-1}; $\Delta H^{\circ} = -25.2$ kJ mol^{-1}; $\Delta S^{\circ}_{298} = -52$ J mol^{-1} K^{-1}). The significant reduction in the negative enthalpy is attributed to the unfavorable geometrical constraints occurring in the chelated form. It is not compensated by an equivalent reduction in the negative entropic term $T\Delta S$ owing to the different stoichiometry of the reaction, so that it leads to a significant decrease in the free energy. The relative populations of chelated versus open structures are well reproduced by theoretical calculations, provided a suitable method is used. As shown in Table 4, at the B3LYP/6-31+G(d,p)//B3LYP/6-31+G(d,p) level, the intramolecular BSSE overstabilizes the chelated structures **1c** and **1b**. In contrast, the LMP2 method predicts "in vacuo" proportions of the chelated and open forms that can be satisfactorily compared to the relative populations found in C_2Cl_4. With this method, the bifurcated structure **1b** proposed by Glaser[25] is calculated in the gas phase as a local minimum (16% of the overall population), 3.4 kJ mol^{-1} higher in energy than the chelated conformer **1c**. Moreover, in this structure **1b**, the O−H···O=C interaction (3.310 Å) appears to be very weak: 26% longer than the sum of van der Waals radii, and the O−H···N hydrogen bond (1.974 Å) is significantly longer than in conformer **1c** (1.926 Å).

We have reported in Table 5 the positions of the two carbonyl absorptions of lobeline base in different solvents and the position of the carbonyl doublet in the simplified fragment model compound: DAPone. The two bands follow a parallel shift in the different solvents. The regular increase in the intensity of the low-frequency component (corresponding to the more polar carbonyl group or to a hydrogen-bonded C=O group) when the solvent polarity increases, indicates the presence of two conformers and confirms the rotational flexibility of the carbonyl

TABLE 5: Solvent Effect on the Carbonyl Doublet of Lobeline Base

compound	solvent	$\nu^1_{(C=O)}$ cm^{-1}	%[a]	$\nu^2_{(C=O)}$ cm^{-1}	%[a]
lobeline	C_6H_{12}	1695.8	54	1689.5	46
	CCl_4	1692.9	51	1685.0	49
	C_2Cl_4	1693.4	45	1686.0	55
	CH_2Cl_2	1688.3	46	1679.3	54
	$CHCl_3$	1688.3	38	1678.5	62
	CH_3CN	1688.6	35	1680.6	65
	$(CH_3)_2SO$	1684.2	23	1677.1	77
DAPone	CCl_4	1690.9	57	1684.3	43

[a] Percentage of band area.

arm already noted by Glaser.[25] However, the suggested association of the hydroxyl group with the carbonyl oxygen in the bifurcated structure **1b** can be excluded by (i) the great similarity of the absorption with the carbonyl doublet of the DAPone model where the OH group is absent and (ii) the increase in the proportion of the low-frequency band in basic solvents (CH_3CN, DMSO) while the OH region shows, on the contrary, that the open form is favored by association with the solvent.

Lobeline Salts. Lobeline salts **2**, **3**, and **4** are soluble enough in dichloromethane to allow a structural analysis in solution by FTIR spectrometry. The characteristic frequencies are shown in Table 6. Contrary to the solid state, the $\nu_{C=O}$ bands observed in dichloromethane are unique with a bandwidth of about 15−17 cm^{-1} suggesting a single conformation of the phenacyl arm of the three salts. The slight asymmetry observed on the low-frequency sides of the carbonyl absorptions (Figure 6B) may be attributed to the presence of a small quantity of associated molecules where the carbonyl groups form weak HB complexes with the solvent. The lack of sensitivity of the carbonyl group frequency toward the formal charge of the nitrogen is striking when the different salts are compared (Table 6). This indicates that, in solution, the ion (N^+)−dipole(C═O) interaction is minimal showing that the carbonyl group is orientated away from the nitrogen (structures **2a**−**4a**), as in the solid-state structures (Figure 3).

The ammonium N^+-H stretching region (Figure 6A) follows the same pattern as in the solid state so that the usual strength of the $N^+H\cdots X^-$ hydrogen bond is conserved in the order: $Cl^- > Br^- > I^-$. Finally, the two ν_{O-H} bands observed in the spectrum (Figure 6A) can be attributed to a free and a hydrogen-bonded conformer (Table 6). In the absence of any accepting nitrogen center available in the protonated molecule, the anion is the HB acceptor site but it may be involved in either an intramolecular or an intermolecular interaction. By successive dilutions (0.036−0.001 mol dm^{-3}) of LobH^+Cl^- solutions, the absorbance ratio of the free and the bonded band intensities decreases only slightly (5.6−4.5). This suggests that, if a low proportion of an intermolecular complex is present in the most concentrated solutions, the major contribution to the associated ν_{O-H} band is due to an intramolecular $O-H\cdots Cl^-\cdots HN^+$ interaction. As noted in Table 6, the frequency shifts $\Delta\nu$(OH) between the free and the bonded OH group are always significantly weaker than the corresponding shifts of methanol on the same anions because the electron densities of the ions are reduced by the first hydrogen bond with the N^+H group.

3. Hydrogen-Bond Basicity of Lobeline. The trifunctional character (Nsp^3, C═O, and OH sites) of lobeline base and the presence of several chelated and unchelated species in solution make the evaluation of the individual affinities extremely complex. We have therefore used different indirect experimental and theoretical methods to partition the global equilibrium constant obtained from the absorbance decrease of *p*NP in carbon tetrachloride. To check the validity of these selected methods we first tested the hypothesis and the procedures on simplified models reproducing the two arms of lobeline.

The Phenacyl Arm: Analysis of *β*-*N*,*N*-Dimethylamino-propiophenone (DAPone). *Association on Propiophenone and Butyrophenone.* The thermodynamics of the association of *p*FP with these two carbonyl compounds are reported in Table 7. Both compounds are found to be slightly less basic than acetophenone ($pK_{HB} = 1.11$).[23] One would have expected a small increase in basicity due to the slight field/polarizability electron-releasing effect of the ethyl and propyl substituent in comparison with the methyl group. Rather, the steric constraint appears as the predominant effect due to the presence of the bulky phenyl substituent. A confirmation of the relative order of basicity is given by the mean electrostatic potential values determined for propiophenone and butyrophenone which are indeed less negative than the acetophenone (Table 1).

Association with DAPone. In DAPone, a molecule mimicking the phenacyl arm of lobeline base, the experimental equilibrium constant (Table 7) must be separated into the individual constants on the nitrogen and the oxygen sites. The carbonyl contribution ($K_{C=O} = 12.2$ dm^3 mol^{-1}) is predicted from eq 4 and the calculated mean $V_{S,min}$ value (−155.0 kJ mol^{-1}). Thus, the HB basicity of the carbonyl group remains very close to the values of the two model compounds of Table 7, despite the presence of a dimethylamino group in β position. In contrast, the nitrogen basicity is significantly disturbed by the presence of the carbonyl group since the calculated value ($K_N = K$(experimental) − $K_{C=O} = 86.5$ dm^3 mol^{-1}) corresponds to a reduction of 41% (0.23 pK_{HB} unit) of the equilibrium constant by comparison with *N*,*N*-dimethylethylamine (Table 7). These findings are in agreement with the large decrease in $V_{s,min}$ on passing from $EtNMe_2$ to DAPone ($\Delta V_{s,min} = 13$ kJ mol^{-1}) and with the respective field effects of the benzoyl and the dimethylamino groups.[47]

The *β*-Hydroxyphenethyl Fragment: Analysis of *β*-*N*,*N*-Dimethylamino-1-phenylpropanol (DAPol). *Association with 1-Phenylpropan-1-ol.* The OH absorption at 3618 cm^{-1} presents an asymmetry due to the benzylic isomerism.[48,49] To prevent its superposition with the OH band of the probe, we used *p*-nitrophenol (*p*NP) as HB donor ($\nu_{OH} = 3595$ cm^{-1}) rather than the standard donor of the pK_{HB} scale,[28] *p*FP ($\nu_{OH} = 3614$ cm^{-1}). The equilibrium constant found for the association *p*NP−phenylpropanol ($K_{pNP} = 18.7$ dm^3 mol^{-1}; log $K_{pNP} = 1.27$) can be converted by means of eq 1 to give p$K_{HB} = 0.71$ ($K = 5.1$ dm^3 mol^{-1}). Owing to the weak electron-withdrawing effect of the phenyl group, phenylpropanol is found to be less basic than propanol ($pK_{HB} = 0.99$; $K = 9.8$ dm^3 mol^{-1}).[24] Compared to benzylalcohol ($pK_{HB} = 0.86$; $K = 7.2$ dm^3 mol^{-1}),[24] phenylpropanol is less basic, indicating that the steric effect of the ethyl substituent overcomes its electron donation by field/polarizability effect.

Association with DAPol. This model of the lobeline hydroxylic arm is also found to be highly chelated in CCl_4 solution. The open form absorbs at 3618 cm^{-1}, and the broad chelated OH band appears at 3244 cm^{-1}. The frequency shift ($\Delta\nu_{OH} = 374$ cm^{-1}), close to the value found for lobeline ($\Delta\nu_{OH} = 359$ cm^{-1}), is a good indication of the validity of this model. This is supported by the thermodynamic parameters of the chelation equilibrium in CCl_4 ($K_{298} = 5.3$; $\Delta G°_{298} = -4.1$ kJ mol^{-1}; $\Delta H° = -15.6$ kJ mol^{-1}; $\Delta S°_{298} = -38.6$ J mol^{-1} K^{-1}) leading to 16% of open form.

TABLE 6: Main IR Absorptions Frequencies (in cm^{-1}) Observed in Lobeline Salts LobH$^+$X$^-$ in Dichloromethane Solution

	ν_{O-H}	$\nu_{O-H\cdots X-}$	$A_{O-H\cdots X}/A_{O-H}$ [a]	$\Delta\nu_{O-H}$ [b]	$\Delta\nu_{O-H}$ [c] MeOH−nBu$_4$N$^+$X$^-$	$\nu_{C=O}$	$\nu_{N^+-H\cdots X-}$
LobH$^+$ Cl$^-$	3597	3309	4.5	288	341	1690	∼2460
LobH$^+$ Br$^-$	3596	3346	3.3	250	286	1690	∼2560
LobH$^+$ I$^-$	3591	3372	1.5	219	237	1690	∼2660

[a] Absorbance ratio of associated and free ν_{O-H} bands. [b] $\Delta\nu_{O-H} = \nu_{O-H} - \nu_{O-H\cdots X^-}$ [c] Frequency shifts of methanol hydrogen bonded to the tetrabutylammonium halogenides in CH_2Cl_2.

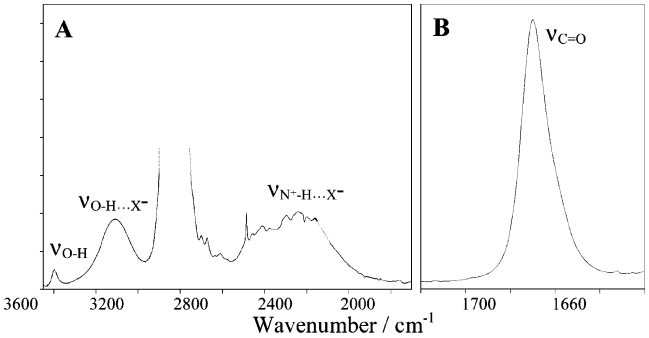

Figure 6. IR Spectrum of lobeline hydrochloride in CH_2Cl_2, in the OH and N$^+$H (A) and the C═O (B) regions.

TABLE 7: Experimental Hydrogen-Bonding Ability of Different Models of the Carbonyl Arm of Lobeline

molecule	K[a]	pK_{HB}	$\Delta G°_{x,298}$[b,c]	$\Delta H°$	$\Delta S°_{x,298}$[b,d]
propiophenone	11.0	1.04	−11.7	−20.3	−29
butyrophenone	11.0	1.04	−11.7	−21.1	−31
DAPone	98.7[e]				
N,*N*-dimethylethylamine [f]	147	2.17	−18.2	−34.7	−54

[a] dm^3 mol^{-1}. [b] Standard state relative to molar fraction units. [c] kJ mol^{-1}. [d] J K^{-1} mol^{-1}. [e] Sum of the two equilibrium constants on the N and C═O sites. [f] Reference 58.

SCHEME 1: Accepting Sites on the Dapol Isomers with Their Estimated Equilibrium Constant with *p*NP[a]

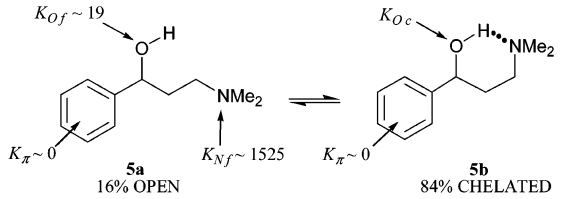

[a] Equilibrium constants in dm^3 mol^{-1}; indexes *c* and *f* refer respectively to the chelated and to the free (open) form.

SCHEME 2: Energy Difference of the Competing Associations of *p*NP with the Chelated Dapol Structure (5b) or through a Bridged Structure (5c)

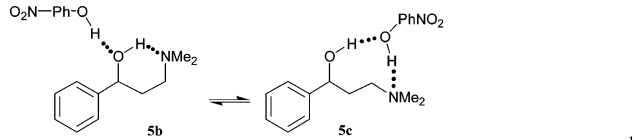

The association of *p*NP with DAPol yields a global equilibrium constant K_t (*p*NP···DAPol) = 537 dm^3 mol^{-1}, which is the sum of several types of association with the two isomers. To build Scheme 1, representing the major sites of complexation of *p*NP in solution, we first neglected the very weak associations of *p*NP with the phenyl rings.[50] Second, we disclosed the existence of a superchelated structure **5c** which appears, by theoretical calculations, about 17 kJ mol^{-1} destabilized toward the complex on conformer **5b** (Scheme 2). Third, by analogy with the previous observations on the phenacyl arm, we

SCHEME 3: Accepting Sites on the Lobeline Isomers with Their Estimated Equilibrium Constant with *p*NP

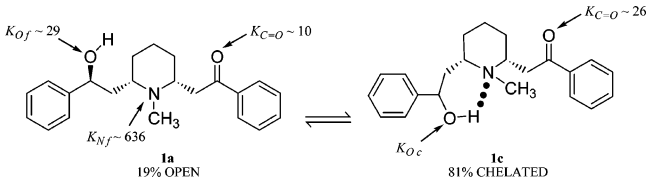

estimated the individual equilibrium constants of the associations of *p*NP with the two basic sites of the open form **5a** on the assumption that the NMe_2 and OH groups have a negligible substituent effect on each other since they are separated by three saturated carbons. Therefore, K_{Of}(*p*NP) ≈ 19 dm^3 mol^{-1} as in 1-phenylpropan-1-ol and K_{Nf}(*p*NP) ≈ 1525 dm^3 mol^{-1} as in *N*,*N*-dimethylethylamine. Confirmation is provided by the very small decrease in the $V_{S,min}$ of the nitrogen on passing from *N*,*N*-dimethylethylamine to open DAPol ($\Delta V_{s,min} = -1.5$ kJ mol^{-1}). It is now possible to write eq 10, the solution of which is the unknown value K_{Oc}(*p*NP) = 345 dm^3 mol^{-1}. It must be noted

$$K_t(p\text{NP}) = 537 = 0.16(1525 + 19) + 0.84K_{Oc}(p\text{NP}) \quad (10)$$

that, owing to the small proportion of the open form, this constant is not greatly affected by intrinsic inaccuracies in the rough estimation of the basicities of its different sites. The evaluated K_{Oc}(*p*NP) constant can, in turn, be converted in the pK_{HB} scale giving pK_{HB} = 1.68. This result is, by far, much greater than the value pK_{HB} = 1.26 obtained for 1-adamantanol, the most basic hydroxylic oxygen of the alcohol family.[24] To check that this equilibrium constant effectively corresponds to structure **5b**, we measured the frequency shift of the *p*FP association on DAPol ($\Delta\nu_{OH}$ (*p*FP) = 324 cm^{-1}) and calculated the minimum electrostatic potential ($V_{S,min} = -171.6$ kJ mol^{-1}) on the oxygen of the chelated hydroxyl. The positions of the coordinates (1.68; 324) and (1.68; 171.6) in the two strongly family dependent pK_{HB}/$\Delta\nu_{OH}$[28] and pK_{HB}/$-V_{S,min}$ plots (Figure 1) definitely confirm the structure of the complex and validate the method of determination of the equilibrium constant. Such an increase in the HB basicity of an oxygen lone pair in a chelated structure has already been observed in the molecule of 2-hydroxyanisole[51] and attributed to the HB cooperativity.[52]

The HB Affinity of (−)-Lobeline. We have reported in Scheme 3 the estimated individual basicities of the different sites in the open **1a** and chelated **1b** form of lobeline. In our estimation (i) the basicities of the hydroxyl and carbonyl oxygen atoms are estimated from eqs 1, and 3,4 and the electrostatic potential mean values reported in Table 4, and (ii) the equilibrium constant of the *p*NP association with the amino nitrogen is calculated from the HB basicity of *N*-methylpiperidine (pK_{HB}= 2.11)[53] assuming that the electron-withdrawing effect of the CH_2COPh substituent reduces the nitrogen basicity by 0.23 pK unit as in DAPone and that the effect of the $CH_2CHOHPh$ arm is negligible as in DAPol. The experimental equilibrium constant of the *p*NP complexation with lobeline

($K_{pNP} = 774$ dm^3 mol^{-1}) can then be partitioned through eq 11 giving $K_{Oc}(pNP) = 771$ dm^3 mol^{-1} ($pK_{HB} = 1.94$).

$$774 = 0.19(29 + 636 + 10) + 0.81(K_{Oc} + 26) \quad (11)$$

As in the DAPol molecule, the oxygen atom of the chelated hydroxyl group is the main contributor to the global HB basicity of the molecule. Moreover, in the lobeline molecule, the stronger internal hydrogen bond gives now a remarkably high HB affinity to the hydroxylic oxygen, equivalent to that of a pyridine nitrogen (pyridine: $pK_{HB} = 1.86$)[54] or an amine nitrogen (triethylamine: $pK_{HB} = 1.98$)[53] Thus, the O−H···N chelation revealed in lobeline, and also in DAPol, generates the most basic hydroxylic oxygen atoms ever measured in the HB basicity scale.

IV. Conclusion

This work shows the great versatility of the lobeline molecule with respect to molecular interactions. Lobeline is able to provide strong internal HBs by means of its OH group in the neutral form and to chelate ions using both the N^+H and OH groups in the protonated form. In low polarity solvents, the chelated structure of neutral lobeline presents an exceptional HB affinity due to the presence of a superbasic hydroxyl oxygen atom. This high HB affinity of the molecule reduces its lipophilicity[31] thus regulating the transport properties of the drug,[55] such as the penetration of the blood-brain barrier.[56,57] When the nitrogen is protonated, the N^+H and the OH groups are found to cooperate, creating an exceptional bidentate HB acidic center, which can favor its docking with different biological receptors.

Acknowledgment. The authors gratefully acknowledge the CCIPL (Centre de Calcul Intensif des Pays de la Loire), the CINES (Centre Informatique National de l'Enseignement Supérieur), and the IDRIS (Institut Des Ressources en Informatique Scientifique) for grants of computer time.

Supporting Information Available: Structural characteristics of neutral lobeline and its hydrochloride and hydrobromide salts; Cartesian coordinates (B3LYP/6-31+G(d,p) level) and electronic energies (LMP2/6-311++G(d,p) level) of lobeline conformers. This material is available free of charge via the Internet at http://pubs.acs.org.

References and Notes

(1) Brejc, K.; van Dijk, W. J.; Klaassen, R. V.; Schuurmans, M.; van der Oost, J.; Smit, A. B.; Sixma, L. K. *Nature* **2001**, *411*, 269.
(2) Hansen, S. B.; Talley, T. T.; Radic, Z.; Taylor, P. *J. Biol. Chem.* **2004**, *279*, 24197.
(3) Celie, P. H. N.; Van Rossum-Fikkert, S. E.; Van Dijk, W. J.; Brejc, K.; Smit, A. B.; Sixma, T. K. *Neuron* **2004**, *41*, 907.
(4) Hansen, S. B.; Sulzenbacher, G.; Huxford, T.; Marchot, P.; Taylor, P.; Bourne, Y. *EMBO J.* **2005**, *24*, 3635.
(5) Graton, J.; Berthelot, M.; Gal, J.-F.; Girard, S.; Laurence, C.; Lebreton, J.; Le Questel, J.-Y.; Maria, P.-C.; Naus, P. *J. Am. Chem. Soc.* **2002**, *124*, 10552.
(6) Graton, J.; Berthelot, M.; Gal, J. F.; Laurence, C.; Lebreton, J.; Le Questel, J. Y.; Maria, P. C.; Robins, R. *J. Org. Chem.* **2003**, *68*, 8208.
(7) Graton, J.; Van Mourik, T.; Price, S. L. *J. Am. Chem. Soc.* **2003**, *125*, 5988.
(8) Arnaud, V.; Berthelot, M.; Le Questel, J.-Y. *J. Phys. Chem. A* **2005**, *109*, 3767.
(9) Arnaud, V.; Berthelot, M.; Evain, M.; Graton, J.; Le Questel, J. Y. *Chem.—Eur. J.*, **2007**, *13*, 1499.
(10) Flammia, D.; Dukat, M.; Damaj, M. I.; Martin, B.; Glennon, R. A. *J. Med. Chem.* **1999**, *42*, 3726.
(11) Felpin, F.-X.; Lebreton, J. *Tetrahedron* **2004**, *60*, 10127.
(12) Cunningham, C. S.; Polston, J. E.; Jany, J. R.; Segert, I. L.; Miller, D. K. *Drug Alcohol Depend.* **2006**, *84*, 211.
(13) Zheng, G.; Dwoskin, L. P.; Crooks, P. A. *J. Org. Chem.* **2004**, *69*, 8514.
(14) Zheng, G.; Dwoskin, L. P.; Deaciuc, A. G.; Norrholm, S. D.; Crooks, P. A. *J. Med. Chem.* **2005**, *48*, 5551.
(15) Damaj, M. I.; Patrick, G. S.; Creasy, K. R.; Martin, B. R. *J. Pharmacol. Exp. Ther.* **1997**, *282*, 410.
(16) Terry, A. V., Jr.; Williamson, R.; Gattu, M.; Beach, J. W.; McCurdy, C. R.; Sparks, J. A.; Pauly, J. R. *Neuropharmacology* **1998**, *37*, 93.
(17) Lendvai, B.; Sershen, H.; Lajtha, A.; Santha, E.; Baranyi, M.; Vizi, E. S. *Neuropharmacology* **1996**, *35*, 1769.
(18) Dwoskin, L. P.; Crooks, P. A. *Biochem. Pharmacol.* **2002**, *63*, 89.
(19) Dwoskin, L. P.; Crooks, P. A.; Jones, M. D. Preparation of cis-2,6-disubstituted piperidines for the treatment of psychostimulant abuse and withdrawal, eating disorders, and central nervous system diseases and pathologies. University of Kentucky Research Foundation. WO/2001/008678, 2001.
(20) Beers, W. H.; Reich, E. *Nature* **1970**, *228*, 917.
(21) Sheridan, R. P.; Nilakantan, R.; Dixon, J. S.; Venkataraghavan, R. *J. Med. Chem.* **1986**, *29*, 899.
(22) Barlow, R. B.; Johnson, O. *Br. J. Pharmacol.* **1989**, *98*, 799.
(23) Besseau, F.; Lucon, M.; Laurence, C.; Berthelot, M. *J. Chem. Soc., Perkin Trans. 2* **1998**, 101.
(24) Laurence, C.; Berthelot, M.; Helbert, M.; Sraidi, K. *J. Phys. Chem.* **1989**, *93*, 3799.
(25) Glaser, R.; Hug, P.; Drouin, M.; Michel, A. *J. Chem. Soc., Perkin Trans. 2* **1992**, 1071.
(26) Compere, D.; Marazano, C.; Das, B. C. *J. Org. Chem.* **1999**, *64*, 4528.
(27) Felpin, F.-X.; Lebreton, J. *J. Org. Chem.* **2002**, *67*, 9192.
(28) Laurence, C.; Berthelot, M. *Perspect. Drug Discovery Des.* **2000**, *18*, 39.
(29) Abraham, M. H.; Grellier, P. L.; Prior, D. V.; Morris, J. J.; Taylor, P. J. *J. Chem. Soc., Perkin Trans. 2* **1990**, 521.
(30) Abraham, M. H.; Grellier, P. L.; Prior, D. V.; Duce, P. P.; Morris, J. J.; Taylor, P. J. *J. Chem. Soc., Perkin Trans. 2* **1989**, 699.
(31) Berthelot, M.; Graton, J.; Ouvrard, C.; Laurence, C. *J. Phys. Org. Chem.* **2002**, *15*, 218.
(32) Arnaud, V.; Le Questel, J.-Y.; Mathe-Allainmat, M.; Lebreton, J.; Berthelot, M. *J. Phys. Chem. A* **2004**, *108*, 10740.
(33) Frisch, M. J.; Trucks, G. W.; Schlegel, H. B.; Scuseria, G. E.; Robb, M. A.; Cheeseman, J. R.; Montgomery, J. A., Jr.; Vreven, T.; Kudin, K. N.; Burant, J. C.; Millam, J. M.; Iyengar, S. S.; Tomasi, J.; Barone, V.; Mennucci, B.; Cossi, M.; Scalmani, G.; Rega, N.; Petersson, G. A.; Nakatsuji, H.; Hada, M.; Ehara, M.; Toyota, K.; Fukuda, R.; Hasegawa, J.; Ishida, M.; Nakajima, T.; Honda, Y.; Kitao, O.; Nakai, H.; Klene, M.; Li, X.; Knox, J. E.; Hratchian, H. P.; Cross, J. B.; Bakken, V.; Adamo, C.; Jaramillo, J.; Gomperts, R.; Stratmann, R. E.; Yazyev, O.; Austin, A. J.; Cammi, R.; Pomelli, C.; Ochterski, J. W.; Ayala, P. Y.; Morokuma, K.; Voth, G. A.; Salvador, P.; Dannenberg, J. J.; Zakrzewski, V. G.; Dapprich, S.; Daniels, A. D.; Strain, M. C.; Farkas, O.; Malick, D. K.; Rabuck, A. D.; Raghavachari, K.; Foresman, J. B.; Ortiz, J. V.; Cui, Q.; Baboul, A. G.; Clifford, S.; Cioslowski, J.; Stefanov, B. B.; Liu, G.; Liashenko, A.; Piskorz, P.; Komaromi, I.; Martin, R. L.; Fox, D. J.; Keith, T.; Al-Laham, M. A.; Peng, C. Y.; Nanayakkara, A.; Challacombe, M.; Gill, P. M. W.; Johnson, B.; Chen, W.; Wong, M. W.; Gonzalez, C.; Pople, J. A. *Gaussian 03*, revision D.02; Gaussian, Inc.: Wallingford, CT, 2004.
(34) *Jaguar*, version 6.0; Schrödinger, L.L.C.: New York, 2005.
(35) Jensen, F. *Introduction to Computational Chemistry*; Wiley: New York, 1999.
(36) Saebo, S.; Tong, W.; Pulay, P. *J. Chem. Phys.* **1993**, *98*, 2170.
(37) Hagelin, H.; Murray, J. S.; Brinck, T.; Berthelot, M.; Politzer, P. *Can. J. Chem.* **1995**, *73*, 483.
(38) Graton, J.; Laurence, C.; Berthelot, M.; Le Questel, J.-Y.; Besseau, F.; Raczynska, E. D. *J. Chem. Soc., Perkin Trans. 2* **1999**, 997.
(39) Ouvrard, C.; Lucon, M.; Graton, J.; Berthelot, M.; Laurence, C. *J. Phys. Org. Chem.* **2004**, *17*, 56.
(40) Schaftenaar, G.; Noordik, J. H. *J. Comput. Aided Mol. Des.* **2000**, *14*, 123.
(41) Graton, J.; Besseau, F.; Berthelot, M.; Raczynska, E. D.; Laurence, C. *Can. J. Chem.* **2002**, *80*, 1375.
(42) Chenon, B.; Sandorfy, C. *Can. J. Chem.* **1958**, *36*, 1181.
(43) Fernandez Bertran, J.; Ballester, L.; Dobriahalova, L.; Sanchez, N.; Arrieta, R. *Spectrochim. Acta, Part A* **1968**, *24*, 1765.
(44) Berthelot, M.; Chabanel, M.; Laurence, C. *Spectrochim. Acta, Part A* **1976**, *32A*, 1771.
(45) Bondi, A. *J. Phys. Chem.* **1964**, *68*, 441.
(46) Hartman, K. O.; Carlson, G. L.; Witkowski, R. E.; Fateley, W. G. *Spectrochim. Acta, Part A* **1968**, *24*, 157.
(47) Hansch, C.; Leo, A.; Taft, R. W. *Chem. Rev.* **1991**, *91*, 165.
(48) Oki, M.; Iwamura, H. *Bull. Chem. Soc. Jpn.* **1959**, *32*, 950.

(49) Mons, M.; Robertson, E. G.; Simons, J. P. *J. Phys. Chem. A* **2000**, *104*, 1430.
(50) Besseau, F.; Laurence, C.; Berthelot, M. *Bull. Soc. Chim. Fr.* **1996**, *133*, 381.
(51) Berthelot, M.; Laurence, C.; Foucher, D.; Taft, R. W. *J. Phys. Org. Chem.* **1996**, *9*, 255.
(52) Kleeberg, H.; Klein, D.; Luck, W. A. P. *J. Phys. Chem.* **1987**, *91*, 3200.
(53) Graton, J.; Besseau, F.; Berthelot, M.; Raczynska, E. D.; Laurence, C. *Can. J. Chem.* **2002**, *80*, 1375.
(54) Berthelot, M.; Laurence, C.; Safar, M.; Besseau, F. *J. Chem. Soc., Perkin Trans. 2* **1998**, 283.
(55) Abraham, M. H.; Chadha, H. S.; Martins, F.; Mitchell, R. C.; Bradbury, M. W.; Gratton, J. A. *Pestic. Sci.* **1999**, *55*, *78.*
(56) Abraham, M. H.; Chadha, H. S.; Mitchell, R. C. *J. Pharm. Sci.* **1994**, *83*, 1257.
(57) Reavill, C.; Walther, B.; Stolerman, I. P.; Testa, B. *Neuropharmacology* **1990**, *29*, 619.
(58) Graton, J.; Berthelot, M.; Besseau, F.; Laurence, C. *J. Org. Chem.* **2005**, *70*, 7892.